

# Characterization of three-color CARS in a two-pulse broadband CARS spectrum

Young Jong Lee,<sup>1,2</sup> Yuexin Liu,<sup>1</sup> and Marcus T. Cicerone<sup>1,3</sup>

<sup>1</sup>Polymers Division, National Institute of Standards and Technology, Gaithersburg, Maryland 20899, USA

<sup>2</sup>yjlee@nist.gov

<sup>3</sup>cicerone@nist.gov

Received September 10, 2007; revised October 19, 2007; accepted October 25, 2007;  
posted October 29, 2007 (Doc. ID 87346); published November 14, 2007

We demonstrate that a broadband coherent anti-Stokes Raman scattering (CARS) spectrum generated with a typical two-pulse scheme contains two distinct, significant signals: “2-color” CARS, where the pump and probe are provided by a narrowband pulse and the continuum pulse constitutes the Stokes light, and “3-color” CARS, where the pump and Stokes are provided by two different frequency components in the continuum pulse and the narrowband pulse serves as the probe. The CARS spectra from the two different mechanisms show distinct characteristics in Raman shift range, laser power dependence, and chirping dependence. We discuss the potential for a 3-color CARS signal to cover the fingerprint region with reduced photodamage of live cells. Official contribution of the National Institute of Standards and Technology; not subject to copyright in the United States.

OCIS codes: 300.6230, 300.6450, 140.3330.

Coherent anti-Stokes Raman scattering (CARS) is a four-wave mixing phenomenon that derives its signal from the third-order nonlinear susceptibility of a medium. Several distinct characteristics, including high spatial resolution, high sensitivity, and label-free chemical specificity make CARS microscopy potentially ideal for noninvasively imaging chemically complex systems. There has been an upsurge in CARS microscopy development activity since Zumbusch *et al.* [1] demonstrated a collinear optical configuration in 1999. Since that time, researchers have exploited very well the advantages of single-frequency CARS microscopy, such as high spatial resolution and rapid data acquisition [2]. While single-frequency CARS microscopy is very powerful for spectrally well-separated chemical species, chemical imaging of complex samples such as an intracellular medium will require broadband spectral sensitivity over the “fingerprint” frequency range of 500 to 2000  $\text{cm}^{-1}$ . Methods developed for increased spectral bandwidth include single-pulse [3,4], multiplex [5,6], and broadband [7–9] CARS microscopy techniques. Single-pulse CARS uses a single tailored pulse to generate CARS spectra as broad as 1300  $\text{cm}^{-1}$  through a “3-color” mechanism, which is represented in Fig. 1(a). Multiplex and broadband CARS have the commonality that both techniques use synchronized narrowband and broadband pulses and generate a CARS signal via the “2-color” process depicted in Fig. 1(a). In these approaches the narrowband pulse serves as pump and probe, and the broadband pulse stimulates the Stokes process. Meanwhile, recent reports [9,10] on broadband CARS discuss the “3-color” contribution to the time-delayed broadband CARS spectra, where a continuum pulse impulsively promotes molecules to vibrationally excited states and a delayed narrowband pulse induces CARS emission. However, the relative 2- and 3-color CARS contributions in a 2-pulse multiplex or a broadband CARS spectrum have not been quantitatively characterized. In this Letter we evaluate the

3-color CARS signal generated simultaneously with 2-color CARS in a 2-pulse broadband CARS spectrum by observing separated Raman shift ranges, laser power dependences, and chirping dependences.

The experimental setup of the 2-pulse broadband CARS is similar to our previous arrangement [7,11]. Briefly, as shown in Fig. 1(b), the output of a Ti:sapphire laser oscillator (Mira 900F, Coherent) [12] was split into two parts. 300 mW of the oscillator output was introduced into a photonic crystal fiber

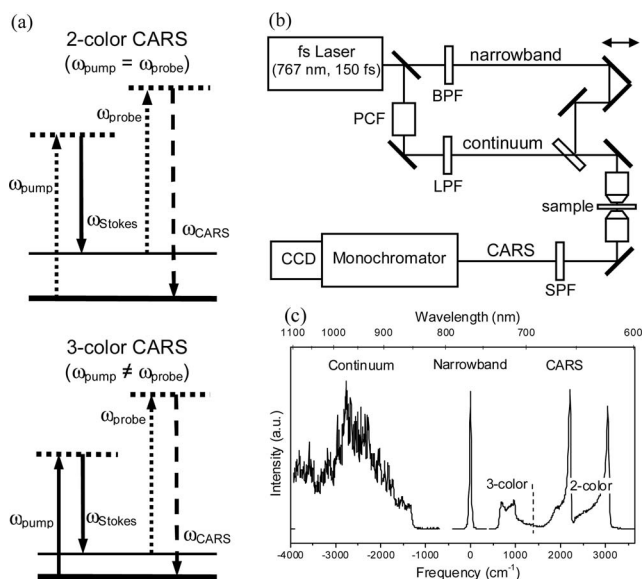


Fig. 1. (a) Energy diagrams of the 2-color and 3-color CARS generation schemes, where the solid arrows indicate the transitions induced by the continuum pulse; the dotted arrows, those induced by the narrowband pulse. (b) Experimental scheme of the 2-pulse broadband CARS system: BPF, bandpass filter; PCF, photonic crystal fiber; LPF, long-pass filter; SPF, short-pass filter. (c) Spectra of continuum and narrowband pulses and a CARS spectrum generated from liquid benzonitrile. The vertical dotted line indicates the low-frequency edge of the 2-color CARS spectrum available with an 850 nm long-pass filter for the continuum.

(Crystal Fibre, Femtowhite) to generate a continuum that is used without pulse compression. The remaining oscillator output light was passed through a bandpass filter ( $\Delta\lambda=1.5$  nm, corresponding to  $\Delta\nu=25$   $\text{cm}^{-1}$ ). The continuum and narrowband beams were focused onto the sample with a 1.3 NA oil immersion objective lens. The generated CARS signal was analyzed by a CCD spectrometer (Roper Scientific, PhotonMax).

Figure 1(c) shows a CARS spectrum of benzonitrile excited using a continuum pulse with no spectral intensity at wavelengths shorter than 850 nm and a narrowband pulse at 767 nm. The anti-Stokes signal at  $<1300$   $\text{cm}^{-1}$  cannot be generated by 2-color CARS because the short-wavelength continuum light is blocked. The spectral bandwidth of the continuum pulse can support impulsive vibrational excitation up to  $1300$   $\text{cm}^{-1}$ , and thus the low-frequency CARS signal could be generated by a 3-color mechanism. Figure 2 gives further evidence for the 3-color mechanism at low Raman shift. In both panels of Fig. 2, the higher-frequency CARS signal shows a clear time-delay dependence of the spectra as a function of pulse temporal separation, which is expected for a 2-color mechanism [13] and reflects the degree of chirp in the broadband pulse [group velocity dispersion (GVD) of approximately  $3 \times 10^4$   $\text{fs}^2$ ]. The low-frequency component has no such time delay dependence, consistent with a 3-color signal generation. Figures 2(a) and 2(b) differ only in that the continuum light is conditioned with an 850 and an 800 nm long-pass filter, respectively. The 2-color CARS signal is extended to lower frequency, and the 3-color signal is extended to slightly higher frequency in Fig. 2(b), as expected under the proposed mechanisms. It is significant that we observe a relatively strong 3-color CARS signal, even with a continuum pulse that has GVD of  $3 \times 10^4$   $\text{fs}^2$ , as ours does. This suggests that many of the broadband CARS spectra in the literature are likely to contain both 2- and 3-color contributions in the low Raman shift region.

The CARS nonlinear polarizations for the 2- and 3-color mechanisms are given by

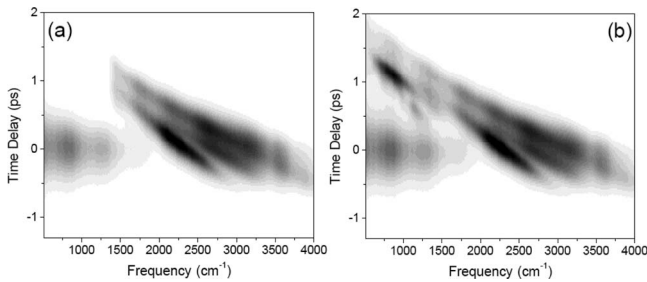


Fig. 2. CARS spectra of a glass coverslip as a function of time delay between the continuum and the narrowband pulses. (a) The wavelength of the continuum is longer than 850 nm, which is equivalent to  $>1300$   $\text{cm}^{-1}$ . (b) The wavelength of the continuum is longer than 800 nm, which is equivalent to  $>500$   $\text{cm}^{-1}$ . The intensity scales are linear and the same in range.

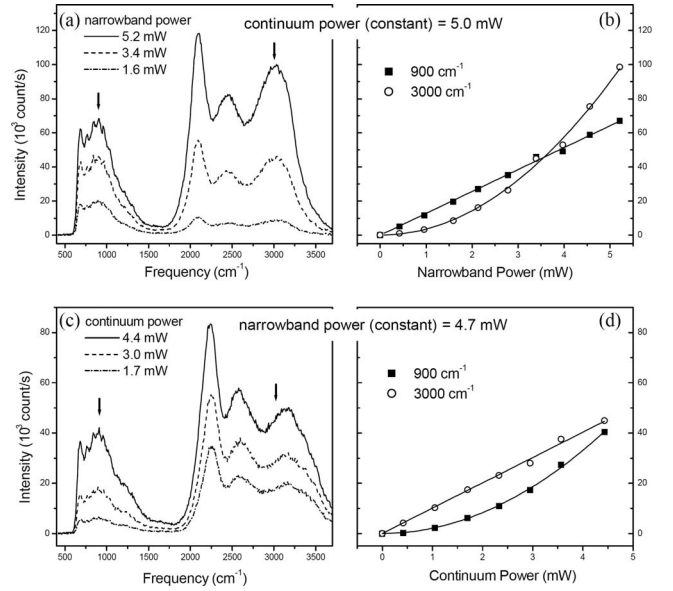


Fig. 3. Laser power dependence of CARS spectra from a glass coverslip. The continuum light is conditioned with an 850 nm long-pass filter. (a) CARS spectra with varying narrowband pulse power and fixed continuum pulse power. (b) CARS intensities at 900 and 3000  $\text{cm}^{-1}$  as a function of power, fitted to linear and quadratic curves, respectively. (c) CARS spectra with varying continuum pulse power and fixed narrowband pulse power. (d) CARS intensities at 900 and 3000  $\text{cm}^{-1}$  as a function of power, fitted to quadratic and linear curves, respectively.

$$P_{3\text{-color}}^{(3)}(\omega_n + \Omega) \propto A(\Omega, \Omega_R, \Gamma) E_n(\omega_n) \times \int_{-\infty}^{\infty} E_c^*(\omega) E_c(\omega + \Omega) d\omega, \quad (1)$$

$$P_{2\text{-color}}^{(3)}(\omega_n + \Omega) \propto A(\Omega, \Omega_R, \Gamma) E_n(\omega_n) E_n(\omega_n)^* E_c(\omega_n + \Omega), \quad (2)$$

where  $E_n$  and  $E_c$  are the narrowband and continuum laser fields, respectively;  $\omega_n$  is the frequency of the narrowband laser;  $\Omega$  is the Raman shift frequency;  $\Omega_R$  is the frequency of the Raman active mode in the medium;  $\Gamma$  is the spontaneous Raman linewidth; and  $A \propto [(\Omega - \Omega_R) + i\Gamma]^{-1}$ . Equations (1) and (2) indicate that the 2- and 3-color CARS signals have different dependences on narrowband and continuum laser pulse powers. Figures 3(a)–3(d) demonstrate a quadratic dependence of the 3-color CARS signal on the continuum power and a linear dependence on the narrowband pulse power, as measured at an anti-Stokes shift of 900  $\text{cm}^{-1}$ . The converse power dependence is observed at 3000  $\text{cm}^{-1}$ , supporting the 2- and 3-color CARS signal generation schemes at the high- and low-frequency range, respectively.

Besides the laser power dependence, Eqs. (1) and (2) suggest that chirp of the continuum pulse affects the spectral range and amplitude of the 2- and 3-color CARS signals differently. The chirping effect of the broadband pulse is demonstrated using a multiplex CARS system [14], which allows better control of dispersion of the femtosecond pulse than the strongly

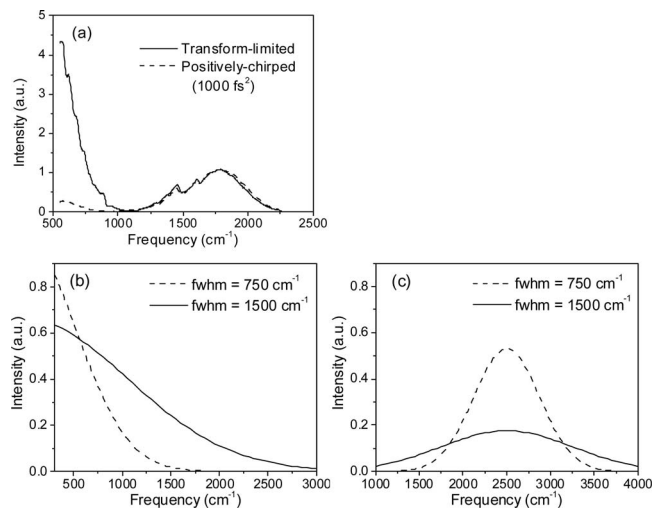


Fig. 4. (a) Chirping effect on 2- and 3-color CARS spectra of 0.5 M benzonitrile in ethanol. The laser powers are 4 and 8 mW at the sample position for the narrowband and the femtosecond pulses, respectively. (b), (c) Pulse width effect of a transform-limited broadband pulse on 3- and 2-color CARS spectra. The time-averaged power  $P$  is adjusted to keep the same photodamage rate, which is assumed to be proportional to  $P^{2.5}/\tau^{1.5}$ .

dispersed multimode continuum light generated from a photonic crystal fiber. Figure 4(a) shows the CARS spectra of a benzonitrile solution excited by femtosecond pulses of different GVD controlled by a prism pair compressor. The 2-color CARS spectrum at the high Raman shift region remains unchanged with increased chirping because the pulse width of the dispersed pulse is still shorter than that of the narrowband pulse. In contrast, the 3-color CARS spectrum at the low Raman shifts shows significant decrease in both signal intensity and spectral range by increasing GVD. This chirping dependence of the 3-color CARS spectrum by a femtosecond pulse with a FWHM of  $500\text{ cm}^{-1}$  and GVD or  $1000\text{ fs}^2$  strongly suggests that optimal compression of the continuum pulse with a broader spectrum ( $\text{FWHM} > 2000\text{ cm}^{-1}$ ) and a greater dispersion ( $\text{GVD} = 3 \times 10^4\text{ fs}^2$ ) can significantly increase the signal intensity and the spectral coverage of the 3-color CARS signal in broadband CARS.

Because CARS is a multiphoton process, the signal intensity becomes stronger when laser pulses have higher peak intensity. However, the high peak intensity of picosecond and femtosecond laser pulses can induce photodamage in live cells, setting limits on signal levels [15–18]. Since the pulse width of the probe pulse cannot be much shorter than Raman linewidths (typically  $\sim 10\text{ cm}^{-1}$ ) for an acceptable ratio of resonant and nonresonant components, we examine the effect of the pulse width of a broadband pulse on 2- and 3-color CARS. Figure 4(c) shows 2-color CARS spectra calculated for transform-limited continuum pulses of 750 and  $1500\text{ cm}^{-1}$  FWHM keeping the same photodamage rate, which is assumed to be proportional to  $P^{2.5}/\tau^{1.5}$  [16], where  $P$  is the time-averaged power and  $\tau$  is the laser pulse width. The shorter continuum pulse exhibits an in-

crease in measurable spectral range but a relatively large decrease in signal intensity. In contrast, the 3-color CARS spectra in Fig. 4(b) exhibit a significant increase in both the signal intensity and the measurable spectral range for the spectrally broader continuum pulse. Thus, 3-color CARS shows the potential to achieve both high signal intensity and a broad Raman spectrum covering the fingerprint region as well as a relatively low photodamage rate of live cells.

In conclusion, we have demonstrated that a 2-pulse broadband CARS spectrum can contain two different CARS generation mechanisms. The 3-color CARS mechanism can be exploited to generate CARS spectra covering the fingerprint region in a way that will minimize potential photodamage effects to live cells.

We thank the National Institutes of Health (NIH 1 R21 EB002468-01) for financial support.

## References

1. A. Zumbusch, G. R. Holtom, and X. S. Xie, *Phys. Rev. Lett.* **82**, 4142 (1999).
2. C. L. Evans, E. O. Potma, M. Puoris'haag, D. Cote, C. P. Lin, and X. S. Xie, *Proc. Natl. Acad. Sci. U.S.A.* **102**, 16807 (2005).
3. D. Oron, N. Dudovich, D. Yelin, and Y. Silberberg, *Phys. Rev. Lett.* **88**, 273001 (2002).
4. S. H. Lim, A. G. Caster, and S. R. Leone, *Phys. Rev. A* **72**, (2005).
5. J. X. Cheng, A. Volkmer, L. D. Book, and X. S. Xie, *J. Phys. Chem. B* **106**, 8493 (2002).
6. M. Muller and J. M. Schins, *J. Phys. Chem. B* **106**, 3715 (2002).
7. T. W. Kee and M. T. Cicerone, *Opt. Lett.* **29**, 2701 (2004).
8. G. I. Petrov, R. Arora, V. V. Yakovlev, X. Wang, A. V. Sokolov, and M. O. Scully, *Proc. Natl. Acad. Sci. U.S.A.* **104**, 7776 (2007).
9. H. Kano and H. Hamaguchi, *J. Raman Spectrosc.* **37**, 411 (2006).
10. K. B. Shi, P. Li, and Z. W. Liu, *Appl. Phys. Lett.* **90**, (2007).
11. T. W. Kee, H. X. Zhao, and M. T. Cicerone, *Opt. Express* **14**, 3631 (2006).
12. Certain equipment is identified in this Letter to specify adequately the experimental details. Such identification does not imply recommendation by the National Institute of Standards and Technology, nor does it imply that the equipment is necessarily the best available for this purpose.
13. K. P. Knutsen, B. M. Messer, R. M. Onorato, and R. J. Saykally, *J. Phys. Chem. B* **110**, 5854 (2006).
14. The multiplex CARS system consists of two synchronized femtosecond lasers. A 60 nm FWHM femtosecond pulse centered at 890 nm from one laser (Halcyon, KMLaser Inc.) was introduced to the focusing objective lens after a prism pair compressor. From the other femtosecond laser (Mira 900F, Coherent), a narrowband pulse was prepared by a dispersionless filter.
15. K. Konig, *J. Microsc.* **200**, 83 (2000).
16. A. Hopt and E. Neher, *Biophys. J.* **80**, 2029 (2001).
17. V. V. Yakovlev, *J. Raman Spectrosc.* **34**, 957 (2003).
18. Y. Fu, H. F. Wang, R. Y. Shi, and J. X. Cheng, *Opt. Express* **14**, 3942 (2006).